Comparison of Torque-speed Characteristics of Interior-magnet Machines in Brushless AC and DC Modes for EV/HEV Applications

Z. Q. Zhu [1], Y. F. Shi [2], and D. Howe [3]

[1] *Department of Electronic and Electrical Engineering, University of Sheffield, Z.Q.Zhu@sheffield.ac.uk*
[2] *Department of Electronic and Electrical Engineering, University of Sheffield*
[3] *Department of Electronic and Electrical Engineering, University of Sheffield*

Abstract

The torque-speed characteristics of an interior magnet brushless motor are compared with particular reference to the flux-weakening performance for EV/HEV applications, when it is operated in brushless AC (BLAC) mode, with 3-phase, sinusoidal current waveforms, and in brushless DC (BLDC) mode with both 2-phase, 120° conduction and 3-phase, 180° conduction rectangular current waveforms. It is shown that while 2-phase, 120° BLDC operation results in the highest torque capability for the same peak current and BLAC operation results in the highest specific torque per rms current when operating below the base-speed, 3-phase, 180° BLDC operation generally results in the best performance in the flux-weakening region.

Keywords

brushless ac, brushless dc, electric vehicle, flux weakening, permanent magnet machine

1. INTRODUCTION

Permanent magnet (PM) brushless machines which are used in the power trains of electric vehicles (EV) and hybrid electric vehicles (HEV) are required to operate in both constant torque and flux-weakening operation modes. PM brushless machines having an interior permanent magnet (IPM) rotor offer potential advantages, in terms of exhibiting a saliency torque, having a higher demagnetization withstand capability, and facilitating extended speed operation. In general, PM machines can be classified as being either brushless DC, with essentially rectangular phase current waveforms, or brushless AC, with essentially sinusoidal phase current waveforms. Generally, BLDC operation is preferred for motors having trapezoidal back-emf waveforms, with BLAC operation being preferred for motors having sinusoidal back-emf waveforms, since this reduces the torque ripple. The steady-state performance of both BLAC and BLDC machines, in both the constant torque and constant power (flux-weakening) regions, has been studied extensively [Pillay et al., 1991; Jahns, 1994; Safi et al., 1995; Jahns, 1984; Jahns, 1987; Morimoto et al., 1994]. Vector control is readily applied to BLAC machines to achieve maximum torque per ampere below base-speed and optimum flux-weakening performance above base-speed [Jahns, 1994; Jahns, 1987; Morimoto et al., 1994; Bose, 1988; Bose, 1988]. Similarly, for BLDC machines, maximum torque per ampere and extended speed operation is realized by advancing the commutation angle, in both 2-phase, 120° (BLDC-120) and 3-phase, 180° (BLDC-180) conduction modes [Safi et al., 1995; Jahns, 1984]. However, the investigations in [Safi et al., 1995; Jahns, 1984] are restricted to surface-mounted magnet, trapezoidal back-emf machines. A comparison of the relative merits of employing the forgoing modes of operation to a PM brushless machine having an interior permanent magnet rotor and a sinusoidal back-emf waveform, particularly in the flux-weakening region, have not been reported in the literature. Thus, in this paper, the torque-speed characteristics of a machine having an IPM rotor and an essentially sinusoidal back-emf waveform are determined experimentally when it is operated as a BLAC, BLDC-120, and BLDC-180 motor in the constant torque and flux-weakening modes, on the basis of (i) the same peak phase current, (ii) the same torque in the constant torque operating region, and (iii) the same rms phase current.

2. BRUSHLESS AC AND DC OPERATION

The IPM motor on which the three different operational modes are to be evaluated has a sinusoidal back-emf waveform, Figure 1. Its parameters are given in Table 1 and the base-speed is around 1750rpm. The detailed control strategy for BLAC operation and BLDC-120 and BLDC-180 are described in Appendix. It should be mentioned that the experimental motor is a small machine and is employed for convenience of investigation although the conclusions should be generally applicable.

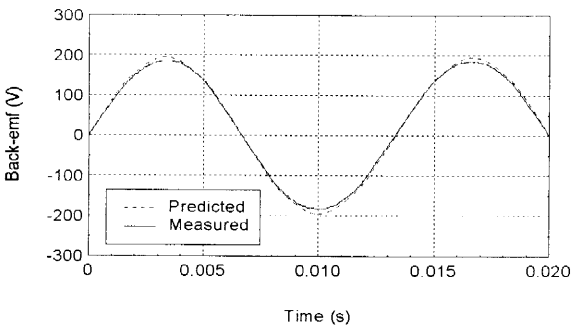

Fig. 1 Finite element predicted and measured line back-emf waveform, 1500rpm.

Table 1 Parameters of IPM brushless machine

DC-link voltage (V_{dc})	285 *V*
Rated torque (T_e)	4.0 *Nm*
Current (peak) ($I_{a\max}$)	4.0 *A*
Phase resistance (R)	8.5 Ω
d-axis inductance (L_d)	$31.2-0.7I_d$ *mH*
q-axis inductance (L_q)	$55-3.7(I_q-1.5)$ *mH*
Number of pole-pairs (p)	3
Flux-linkage ($\psi_m = E/\omega_e$)	0.227 W_b

2.1 Brushless AC operation, BLAC

In the constant torque mode, optimal d-q axis current profiles for maximum utilization of the saliency torque are imposed for maximum torque per ampere, whilst in the constant power mode optimal current profiles are imposed according to the supply voltage and current constraints [Morimoto et al, 1994].

The torque-speed characteristics which result both with and without flux-weakening control are shown in Figure 2, together with the optimal phase advance angle β_0, the leading angle of current vector from q-axis and $\beta_0 = \arctan(-I_d/I_q)$. Figure 3 and Figure 4 show typical phase current waveforms when the machine is running below

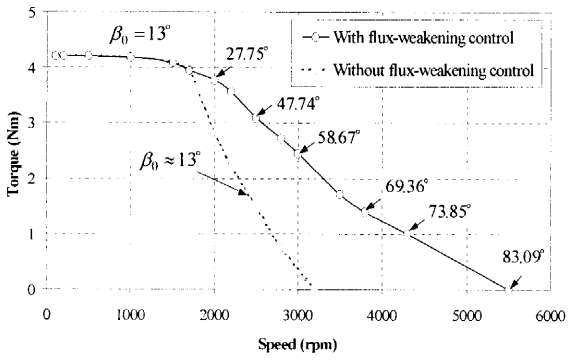

Fig. 2 Measured torque-speed characteristics for BLAC operation.

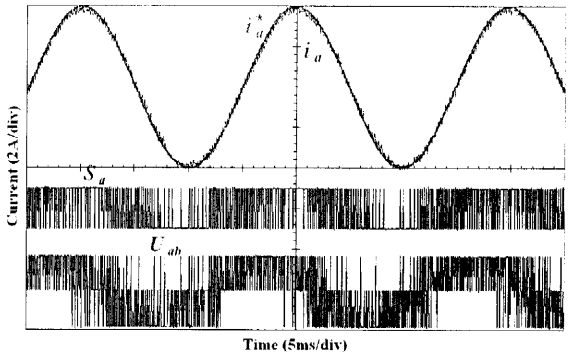

Fig. 3 Phase current waveforms for BLAC operation below base-speed, 1000rpm. S_a: gate drive signal; U_{ab}: line voltage; i^*_a: demand Phase A reference current; i_a: actual Phase A current

and above base-speed, both with and without flux-weakening control. As can be seen, below base-speed, a fixed phase advance angle (13°) is employed to utilize the saliency torque (this is also applied above base-speed even when 'without flux-weakening', Figure 2 and Figure 4 (a)). As expected, above base-speed, the current and torque performance is significantly improved by employing flux-weakening control.

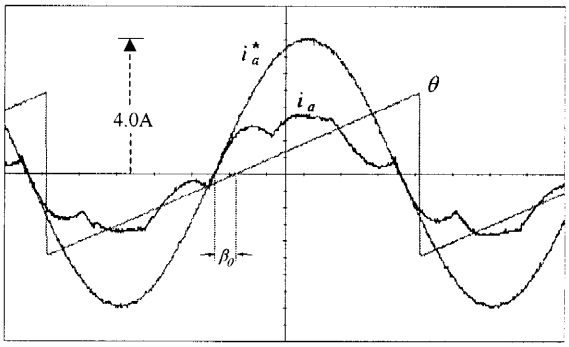

(a) Without flux-weakening

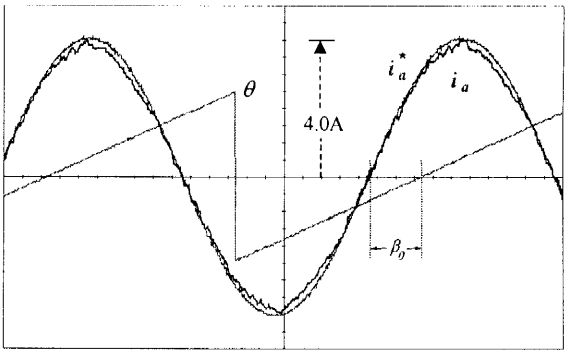

(b) With optimal flux-weakening

Fig. 4 Phase current waveforms for BLAC operation above base-speed, 2500rpm. i^*_a: demand Phase A reference current; i_a: actual Phase A current

2.2 Brushless DC operation with 2-phase, 120° conduction, BLDC-120

Figure 5 shows typical measured phase current waveforms for different commutation advance angles when running below and above base-speed, the maximum current being limited to 4A. As shown in Figure 6, $\theta_c = 0°$ corresponds to the instant at which the phase winding is switched on lagging 30° behind the zero-crossing of the back-emf waveform ($\theta = 0$). Thus, $\theta_c = 30°$ corresponds to the commutation coinciding with the zero-crossing of the back-emf. In general, at low speed, Figure 5 (a), due to 2-phase conducting operation mode, the phase current is discontinuous. However, during the commutation period, all three phases conduct due to the circulating current via the freewheel diode. The phase current waveform may become continuous at high speed, particularly under flux-weakening control, Figure 5 (b). Hence, unlike in BLAC operation mode, the angle, β_0, by which the zero-crossing of phase current waveform leads the zero-crossing of the back-emf waveform, may be different from the commutation advance angle, θ_c, as illustrated in Figure 6. The influence of commutation advance angle θ_c on torque-speed and RMS phase current characteristics is shown in Figure 7. As can be seen,

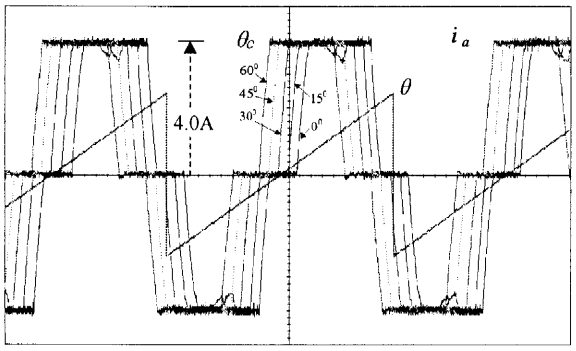

(a) 1000rpm

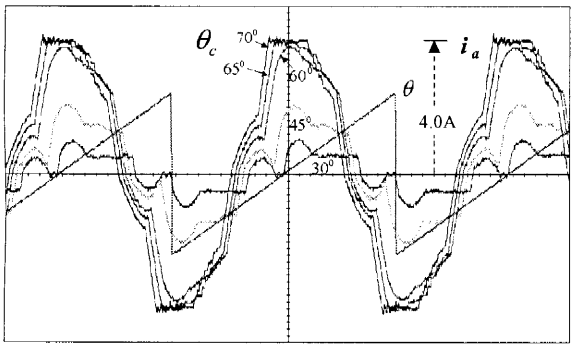

(b) 2500rpm

Fig. 5 Measured phase current waveforms at different commutation advance angles for BLDC-120 operation

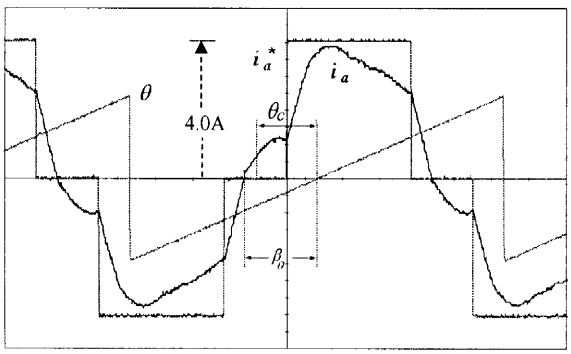

Fig. 6 Demand and actual phase current waveforms and rotor position. BLDC-120, 2500rpm, θ_c=60°, $\beta_0 \approx 72°$

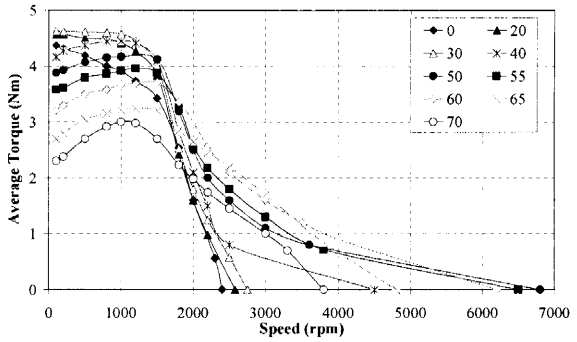

(a) Influence of commutation advance angle θ_c on torque-speed characteristics

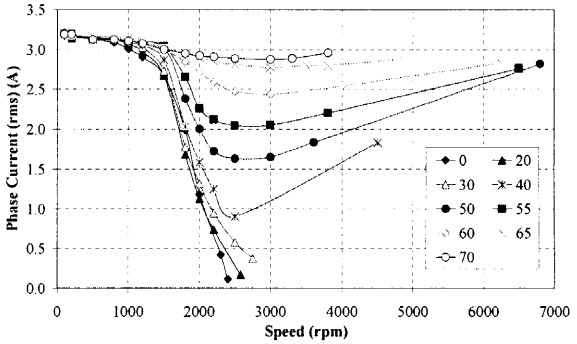

(b) Influence of commutation advance angle θ_c on RMS phase current-speed characteristics

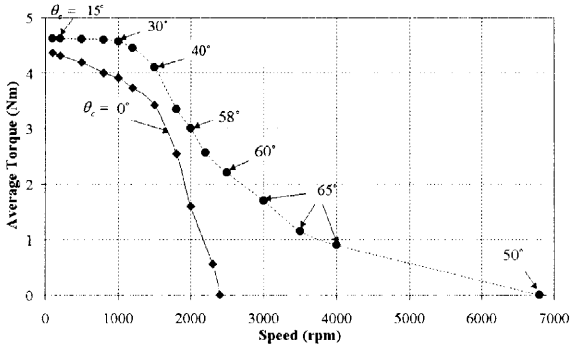

(c) Optimal commutation advance angle and maximum torque-speed

Fig. 7 Measured torque-speed characteristics for BLDC-120 operation

by advancing the commutation angle, the rated current is more or less maintained and the torque is enhanced at high speed. The optimal commutation advance angle for maximum torque is speed dependent and can be obtained experimentally (or by simulation).

2.3 Brushless DC operation with 3-phase, 180° conduction, BLDC-180

In this case, three phases are always conducting. θ_c =0° now corresponds to a phase winding being excited at the zero-crossing of its back-emf waveform (θ = 0). Figure 8 shows measured phase current waveforms for different commutation advance angles, again when the motor is running below and above base-speed and with the maximum current limited to 4A. Similar to the case of BLDC-120 operation mode, the angle, β_0, by which the zero-crossing of phase current waveform leads the zero-crossing of the back-emf waveform, may be different from the commutation advance angle, θ_c, as illustrated in Figure 9. The influence of commutation advance angle θ_c on torque-speed and RMS phase current characteristics, as well as the optimal commutation advance angle and the resulting maximum torque per ampere-speed characteristic is shown in Figure 10. Similar to the case of BLDC-120, by advancing the commutation angle, the rated current is more or less maintained and the torque is enhanced at high speed, while the op-

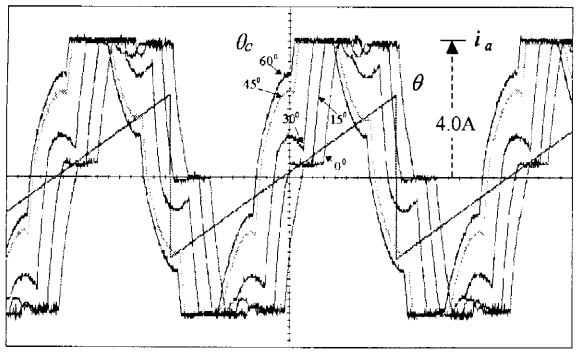

(a) 1000rpm

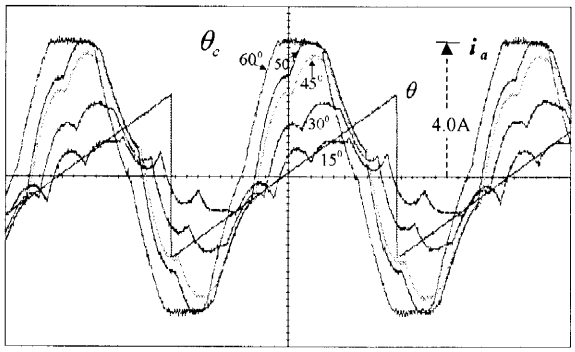

(b) 2500rpm

Fig. 8 Measured phase current waveforms at different commutation advance angles for BLDC-180 operation

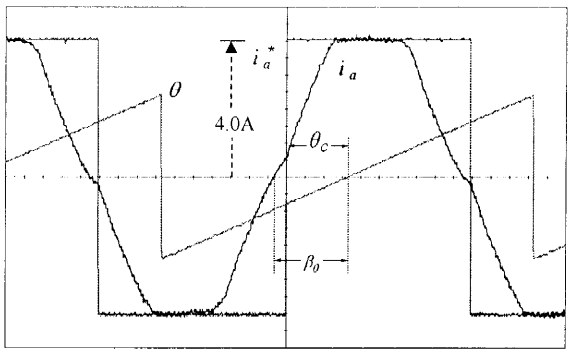

Fig. 9 Demand and actual phase current waveforms and rotor position. BLDC-180, 2500rpm, θ_c=60°, $\beta_0 \approx$ 75°

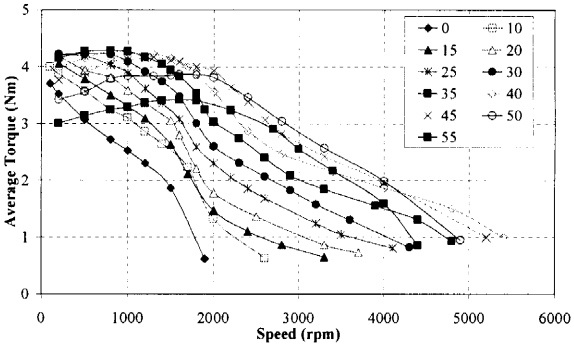

(a) Influence of commutation advance angle θ_c on torque-speed characteristics

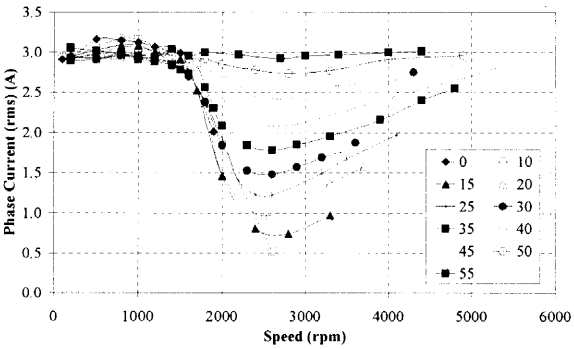

(b) Influence of commutation advance angle θ_c on RMS phase current-speed characteristics

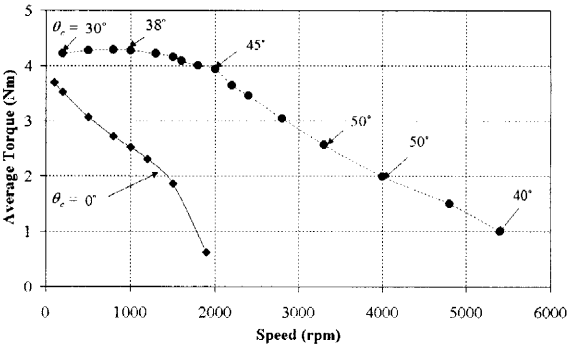

(c) Optimal commutation advance angle and maximum torque-speed

Fig. 10 Measured torque-speed characteristics for BLDC-180 operation

timal commutation advance angle for maximum torque is speed dependent.

As will be evident, in both BLDC operating modes the phase current waveforms are far from being rectangular or sinusoidal, only the fundamental component contributing to the average torque and harmonics resulting in torque ripple, since the back-emf waveform is sinusoidal. However, since the zero-crossing of the current waveform varies with speed, the phase angle β_0, which is defined similarly as for a BLAC drive, cannot be controlled directly, since, for a given θ_c, β_0 varies with both the speed and the torque. Further, while the optimal value of θ_c increases with the speed up to ~4000rpm, above this speed the optimal value of θ_c reduces due to the varying phase angle β_0 between the current and the back-emf, as will be evident from Figure 5 and Figure 8, in which it can be seen that at high speed with optimal flux-weakening control the phase current waveforms in both BLDC operating modes become more sinusoidal since the high order current harmonics are suppressed by their higher reactance as the speed increases. In addition, at high rotational speeds, over-currents are observed in the phase current waveforms, as can be seen in Figure 11 and Figure 12. These are uncontrollable since they are due to circulating currents which flow via the freewheel diodes during commutation.

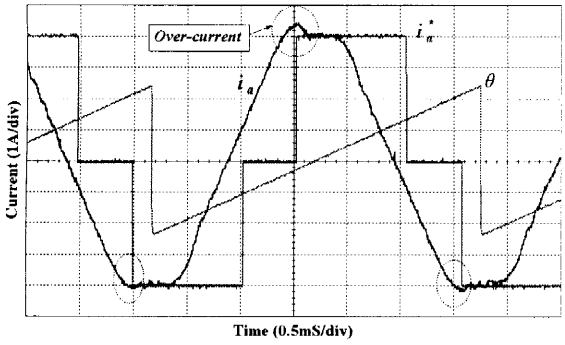

Fig. 11 Phase currents for BLDC-120 operation, 6500rpm, $\theta_c = 50°$

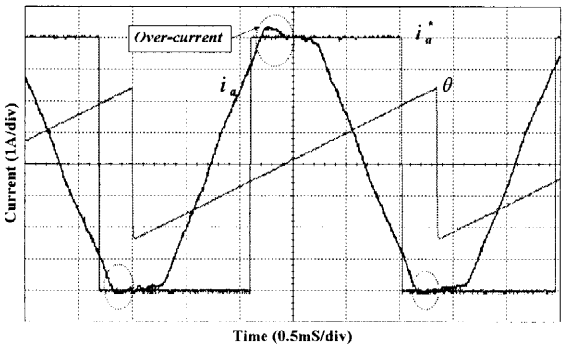

Fig. 12 Phase currents for BLDC-180 operation, 7050rpm, $\theta_c = 40°$

3. PERFORMANCE COMPARISON

The torque-speed characteristics which result when the motor is operated in BLAC, BLDC-120 and BLDC-180 modes are compared on the basis of (i) the same peak phase current (Case #1), (ii) the same torque in the constant torque region (Case #2), and (iii) the same rms phase current (Case #3).

Figure 13 shows the torque-speed characteristics for BLAC and BLDC-120 operation. As will be seen from Figure 13 (a), BLAC operation results in superior flux-weakening performance, while the maximum torque is higher with BLDC-120 operation for the same peak phase current (Case #1), since the fundamental current is the highest. However, if the performance is judged on the basis of the specific torque per rms current, BLAC operation is superior throughout the operating speed range.

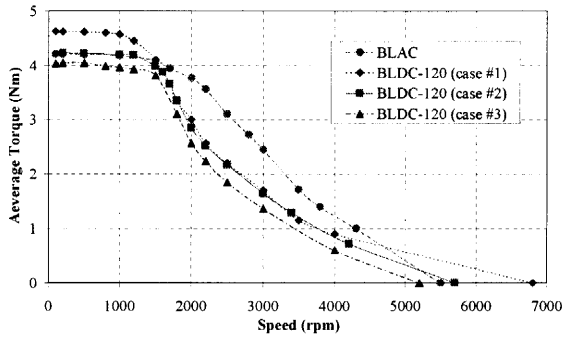

(a) Average torque

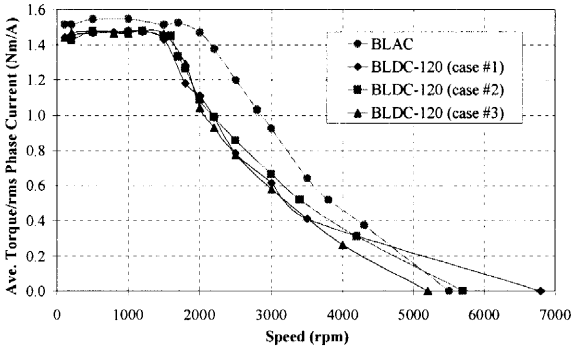

(b) Average torque/measured RMS current

Fig. 13 Torque-speed characteristics for BLAC and BLDC-120 operation

Figure 14 compares the torque-speed characteristics which result with BLAC, BLDC-120 and BLDC-180 operation and the same peak phase current (Case #1). As will be seen from Figure 14 (a), due to its high fundamental current, BLDC-120 operation again results in the highest torque capability below base-speed, while BLDC-180 operation results in the highest torque in the

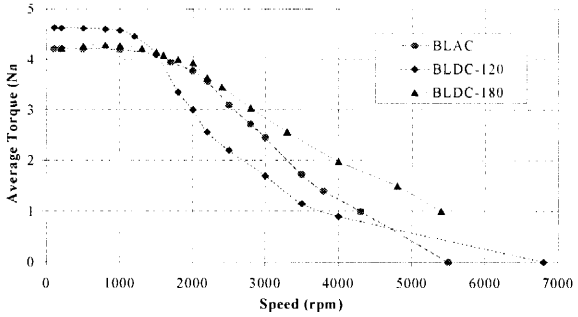

(a) Average torque

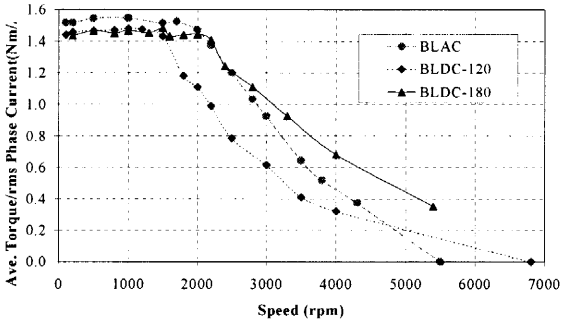

(b) Average torque/measured RMS current

Fig. 14 Torque-speed characteristics for brushless BLAC and BLDC operation (Case #1)

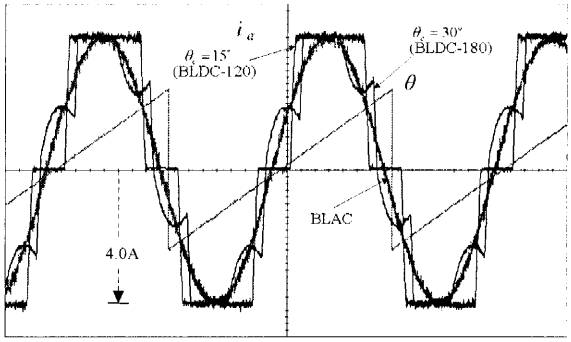

(a) 500rpm

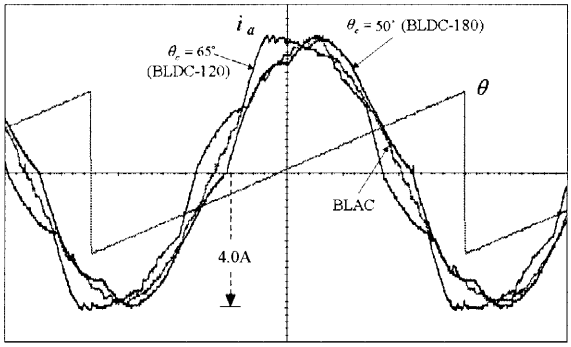

(b) 3000rpm

Fig. 15 Phase current waveforms for BLAC and BLDC operation (Case #1)

flux-weakening region since its DC link voltage utilization is the highest. However, when the performance is judged on the basis of the specific torque per rms current, BLAC operation is superior below base-speed, while BLDC-180 operation remains superior in the flux-weakening region.

Figure 15 shows representative phase current waveforms when the motor is operated in all three modes, in both the constant torque and flux-weakening regions, with the phase currents constrained to have the same peak value (Case#1). As will be seen, in the BLDC-120 and BLDC-180 operating modes the current waveforms become more sinusoidal as the speed is increased since the high order current harmonics are suppressed by their higher reactance, as mentioned before, while in the flux-weakening region the fundamental supply voltage and current component is highest in the BLDC-180 operating mode due to the six-step voltage operation. Consequently, it results in the highest torque per rms current capability.

4. CONCLUSIONS

The torque-speed characteristics of an IPM brushless machine when operated as a brushless AC motor and a brushless DC motor, with both 2-phase, 120° conduction and 3-phase, 180° conduction, has been investigated. It has been shown that (a) BLDC-120 operation yields the highest torque capability for the same peak phase current below base speed; (b) BLAC operation yields the highest specific torque per rms current below base-speed; (c) BLDC-120 operation exhibits the poorest flux-weakening performance; (d) BLDC-180 operation generally results in the best performance in the flux-weakening region. Hence, in EV/HEV applications, even for IPM motors which have essentially sinusoidal back-emf waveforms, it may be advantageous to employ BLDC-180 operation in the flux-weakening region, e.g. to employ a hybrid operation mode - BLAC operation in the constant torque region and BLDC-180 operation in the flux-weakening region, for which a transition method proposed in [Bose, 1988; Bose 1988] may be employed. However, other aspects of performance, in terms of efficiency and torque ripple, should also be considered.

References

Bose, B. K., A high-performance inverter-fed drive system of an interior permanent magnet synchronous machine, *IEEE Trans. Ind. Appl.*, Vol. 24, No. 6, 987-997, 1988.

Bose, B. K., A microcomputer-based control and simulation of an advanced IPM synchronous machine drive system for electric vehicle propulsion, *IEEE Trans. Ind. Elect.*, Vol. 35, No. 4, 547-559, 1988.

Jahns, T. M., Flux-weakening regime operation of an interior permanent-magnet synchronous motor drive, *IEEE Trans. Ind. Appl.*, Vol. 23, No. 4, 681-689, 1987.

Jahns, T. M., Motion control with permanent-magnet ac machines, *IEEE Proc.*, Vol. 82, No. 8, 1241-1252, 1994.

Jahns, T. M., Torque production in permanent-magnet synchronous motor drives with rectangular current excitation, *IEEE Trans. Ind. Appl.*, Vol. 20, No. 4, 803-813, 1984.

Morimoto, S., M. Sanada, and Y. Takeda, Wide-speed operation of interior permanent magnet synchronous motors with high-performance current regulator, *IEEE Trans. Ind. Appl.*, Vol. 30, No. 4, 920-926, 1994.

Pillay, P., and R. Krishnan, Application characteristics of permanent magnet synchronous and brushless dc motors for servo drives, *IEEE Trans. Ind. Appl.*, Vol. 27, No. 5, 986-996, 1991.

Safi, S. K., P. P. Acarnley, and A. G. Jack, Analysis and simulation of the high-speed torque performance of brushless dc motor drives, *IEE Proc. -Electr. Power Appl.*, Vol. 142, No. 3, 919-200, 1995.

Zhu, Z. Q., Y. F. Shi, and D. Howe, Influence of DSP controller on performance of a permanent magnet brushless ac drive in flux-weakening mode, *Journal of Zhejiang University Science*, Vol. 6A, No. 2, 83-89, 2005.

Appendix

(a) Control strategy for BLAC drive

The steady-state d-q axis voltage equations for a BLAC motor are:

$$\begin{cases} U_d = RI_d - \omega L_q I_q \\ U_q = RI_q + \omega(\psi_m + L_d I_d) \end{cases} \quad (1)$$

where U_d, U_q, I_d, I_q, L_d, L_q are the d- and q-axis voltages, currents, and inductances, respectively; R is the phase winding resistance; ω is the synchronous electrical angular velocity; and ψ_m is the maximum flux-linkage per phase due to the permanent magnets. The peak phase current and voltage, U_a and I_a, which are limited by the inverter, are:

$$\begin{cases} U_a = \sqrt{U_d^2 + U_q^2} \le U_{\max} \\ I_a = \sqrt{I_d^2 + I_q^2} \le I_{\max} \end{cases} \quad (2)$$

The torque and the power are given by:

$$T = \frac{3}{2} p\left[\psi_m I_q + (L_d - L_q) I_d I_q\right] \quad (3)$$

and $P = (\omega/p)T$ (4)

where p is the number of pole-pairs, I_{max} is the maximum phase current, and U_{max} is the maximum inverter voltage, which can be estimated from the dc-link voltage U_{dc}, viz. $U_{max} = \frac{2}{\pi} U_{dc}$.

In order to simplify the control algorithm, the winding resistance R is first neglected in deriving the relationship between d-q axis currents. However, the resistance voltage drop can be subsequently compensated for by employing a feed-forward compensation scheme, as described in [Zhu et al., 2005].

Therefore,

$$\begin{cases} U_d \approx -\omega L_q I_q \\ U_q \approx \omega L_d I_d + \omega \psi_m \end{cases} \quad (5)$$

For the IPM motor, $L_d < L_q$. Thus, in the constant torque mode (i.e. below the base speed), when maximum torque per ampere control is used:

$$I_d = \frac{\psi_m}{2(L_q - L_d)} - \sqrt{\frac{\psi_m^2}{4(L_q - L_d)^2} + I_q^2} \quad (6)$$

In the flux-weakening mode, the optimal d- and q-axis current profiles are derived from the voltage and current constraints of the inverter:

$$I_d = -\frac{\psi_m}{L_d} + \frac{1}{L_d}\sqrt{\frac{U_{smax}^2}{\omega_e^2} - (L_q I_q)^2} \quad (7)$$

Figure 16 shows a schematic diagram of the vector-controlled BLAC drive based on a TMS320C31 float-point DSP. The torque command T^* is determined from the speed error $\omega^* - \omega$ through a PI controller. The foregoing optimal control strategy is employed to determine the d- and q-axis currents I^*_d and I^*_q as well as the phase advance angle β_0. I^*_q and I^*_d are transformed to the phase currents i^*_a, i^*_b and i^*_c according to the instantaneous rotor position to control the instantaneous torque. The

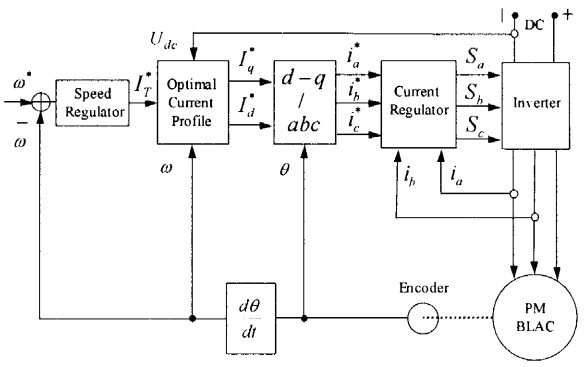

Fig. 16 Schematic diagram of vector-controlled PM BLAC drive

current-controlled PWM inverter is used to force the actual currents i^*_c, i^*_b and i^*_c to follow the demanded currents i^*_a, i^*_b and i^*_c.

(b) Commutation strategies of BLDC drives

A BLDC drive can operate in either 2-phase, 120° conduction, or 3-phase, 180° conduction. The commutation sequences are shown in Figure 18 and Figure 19 for BLDC-120 and BLDC-180, respectively, corresponding to the conventional 3-phase inverter, Figure 17. For simplicity, both BLDC-120 and BLDC-180 are implemented by using TMS320C31 DSP.

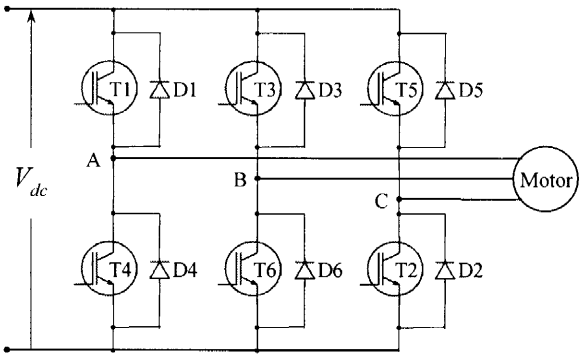

Fig. 17 3-phase inverter for BLAC and BLDC drives

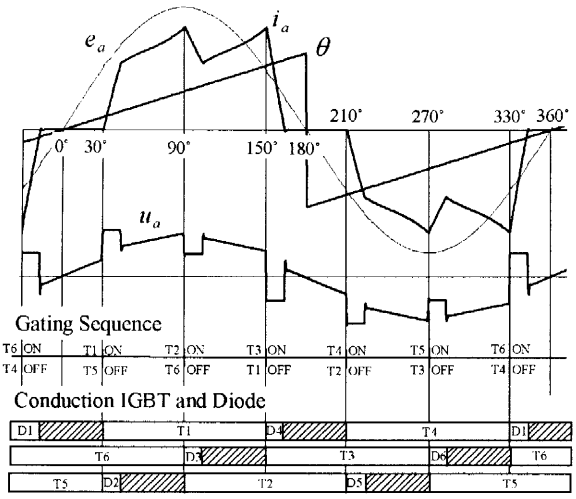

Fig. 18 Commutation strategy, back-emf, current, voltage, gate trigger sequence and rotor position in 2-phase, 120° conduction, BLDC-120 mode ($\theta_c = 0°$)

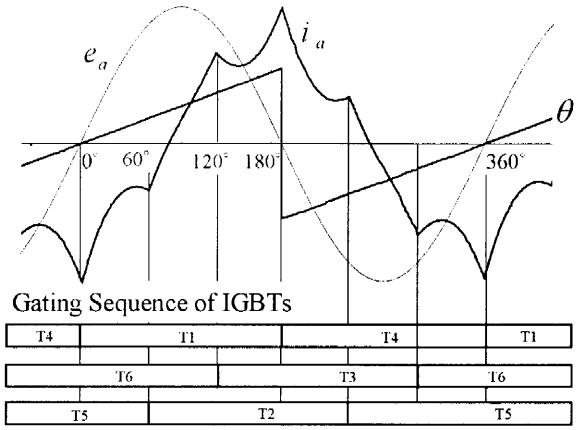

Fig. 19 Commutation strategy, back-emf, current, gate trigger sequence and rotor position in 3-phase, 180° conduction, BLDC-180 mode in BLDC-180 mode ($\theta_c = 0°$)